JACS
JOURNAL OF THE AMERICAN CHEMICAL SOCIETY

Article

Sequence-controlled Stimuli-responsive Single-Double Helix Conversion between 1:1 and 2:2 Chloride-Foldamer Complexes

Yun Liu, Fred C Parks, Wei Zhao, and Amar H Flood

J. Am. Chem. Soc., **Just Accepted Manuscript** • DOI: 10.1021/jacs.8b09899 • Publication Date (Web): 22 Oct 2018

ACS Publications

is published by the American Chemical Society. 1155 Sixteenth Street N.W., Washington, DC 20036

J. AM. CHEM. SOC.

Sequence-controlled Stimuli-Responsive Single-Double Helix Conversion between 1:1 and 2:2 Chloride-Foldamer Complexes

Yun Liu,*[,†,‡] Fred C Parks,[†] Wei Zhao,[†] and Amar H. Flood*[,†]

[†]*Department of Chemistry, Indiana University, 800 E. Kirkwood Avenue, Bloomington, IN 47405, USA*

*E-mail: yl41@indiana.edu, aflood@indiana.edu

ABSTRACT

The primary sequence in biopolymers carries the information to direct folded secondary structures, modulate their stabilities, and control the resultant functions. Our ability to encode such information into non-biological oligomers and polymers, however, is still limited. Here, we describe a C_2 symmetric aryl-triazole foldamer that assembles into a chloride-templated 2:2 double helix and the discovery that its interconversion with the simpler 1:1 single helix can be driven by solvent quality, temperature, and concentration. We use single-site substitutions in the 13-residue sequence (two terminal sites and one central site) to reveal that the stability of the double helix is largely dictated by the differences in the anion binding power between single and double helices as well as the location of the modified residues. Specifically, placement of stabilizing CH•••Cl^- hydrogen bonding interactions at the chain ends in the form of bisamide phenylene residues is found to highly favor the double helix. While the burial of π surfaces and the solvophobic effect also helps to stabilize the double helix, their role was found to be less sensitive to the modifications considered. This understanding of how chemical information is programmed into the primary sequence provides a powerful tool for controlling structure and properties of abiological foldamers.

INTRODUCTION

Nature uses helical structures for information storage and readout. Double helix DNA both stores and relays the genetic information in its sequence, and its high-fidelity interstrand recognition supports sequence-programmable structures to produce next-generation nanoscale materials, like DNA origami.[1-5] Inspired by these functions, synthetic versions of double helices derived from abiological foldamers have been considered as platforms for a range of functions, such as, host-guest recognition,[6-8] molecular switches,[9-15] and self-replicating systems.[16] These behaviors, however, have yet to be correlated to the information contained in the primary sequence. We use single-site substitutions in the linear sequence as an untapped approach to help identify the factors controlling duplex stability and thus to understand an unprecedented mode of switching between single and double helices that rely on *n*:*n* chloride complexation (Figure 1a).

The formation of synthetic double helices typically involves the use of specific interactions.[17] Early examples made use of strong metal-ligand contacts,[18-19] followed by designs bearing direct interstrand interactions, e.g., hydrogen bonds, π-π interactions, and salt bridges.[20] Systems that utilize anion-receptor interactions have also emerged,[21] e.g., bicyclic guanidiniums,[22] iodo-pyridinium ethynylenes,[23] diammonium bis-pyridiniums,[24] isophthalamides,[25] oligo-ureas,[26] oligo-pyrroles,[27-28] and aryl-triazole foldamers,[29] which have all been stabilized with various anions. Solid state forms of these double helices[24-25, 27] are more common than those in solution.[22-23, 26] Futhermore, despite the various examples of single helices that are responsive[30-32] and switchable,[33-35] examples of ion-bound foldamers displaying facile and reversible conversion between double and single helices are unknown, and this is true for either anion- or cation-stabilized helices.

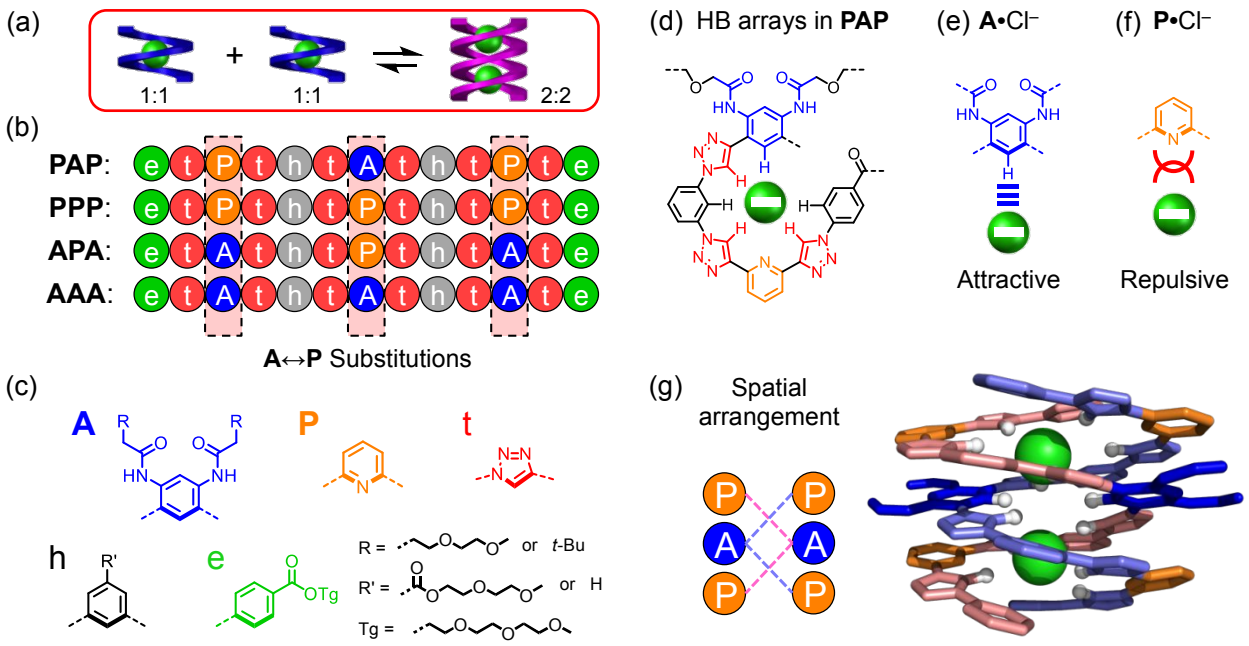

Figure 1. (a) Cartoon representation of the switch between two 1:1 single helix and one 2:2 double helix. (b) Single-site **A↔P** substitutions of aryl-triazole foldamers generate four different sequences: **PAP**, **PPP**, **APA**, and **AAA**. (c) Colour-coded formulae and associated letters of the sequence elements for aryl-triazole foldamers. The inner rim of the helix is marked by thick bonds. (d) Chemical structure of foldamer **PAP** showing an array of hydrogen bond (HB) donors towards the central anion, in which (e) stabilizing and (f) destabilizing interactions are encoded by **A** and **P**, respectively. (g) The organization of sequence elements in the 2:2 **PAP**:Cl^- double helix (DFT-optimized geometry).

A range of design features are known to support double helices. When these helicates involve two anions, strong driving forces, such as charge-assisted halogen bonds[23] or charge-assisted hydrogen bonds,[22] have been used and presumably help offset charge-charge repulsions. These add to the growing examples of receptors capable of recognizing multiple anions[36-41] in a well-defined fashion.[21] In cases of guest-free double helices, hydrophobic driving forces can be

used in which the burial of π surfaces is greater in double helices than singles.[42] In either case, use of longer aromatic moieties better accomodates smaller torsion angles to help lower strain in the double helices.[43] Residues that support additional π-π contacts external to the main chain can also enhance stability in polar solvents.[44] To complement these prior works, we present a novel sequence that is both capable of encoding a multitude of noncovalent interactions and which is readily modifiable. We seek to use sequence variation as a means to test and then reveal how the driving forces encoded into the foldamer's primary sequence are responsible for the secondary structure and for the emergent switching properties.

Encouraged by recent work showing that sequence variation can control the shapes of abiological helices[45-46] and host-binding cavities,[47] we use single-site substitutions (Figure 1b–c) to understand the identity and location of residues to modify in order to control the stability of double helices. This approach was undertaken in an effort to help rationalize the discovery, reported herein, of a novel stimuli-responsive switch (Figure 1a) between a 2:2 foldamer-anion duplex and a 1:1 single helix. Furthermore, while the aryl-triazole foldamers we used (Figure 1d) are known to form double helices,[29] they are discovered for the first time to form complexes with two chloride anions instead of just one ion. The presence of two anions inside the double helix alters the admixture of driving forces defined by the foldamer's linear sequence. This knowledge of how driving forces can be altered by the content of the primary sequence will eventually allow for the emergence of tailored structures and functions in abiological foldamers.

RESULTS AND DISCUSSION

Design and Synthesis. The 13-subunit foldamers incorporate six triazoles and seven aryls in an alternating aryl-triazole sequence. The triazoles serve as both inter-aryl linkers and

the principal hydrogen bonding residues for stabilizing chloride anions using CH donors:[48-53] CH•••Cl⁻. There are four types of aryl units: pyridyl (**P**, orange), bisamide-functionalized phenylene (**A**, blue), bridging *meta*-phenylenes (h, gray), and end capping *para*-phenylenes (e, green). The bisamide phenylene and pyridyl groups were varied in our studies. They confer opposite characteristics (Figure 1e and f) upon the foldamer for anion binding: the electron withdrawing amides on the phenylene polarize the CH donors and produce a large 8-D dipole moment to stabilize anions, while pyridyl displays a 3-D dipole and a lone pair that destabilize anions.

Scheme 1. Synthesis of the Central (top) and Terminal (bottom) Building Blocks[a]

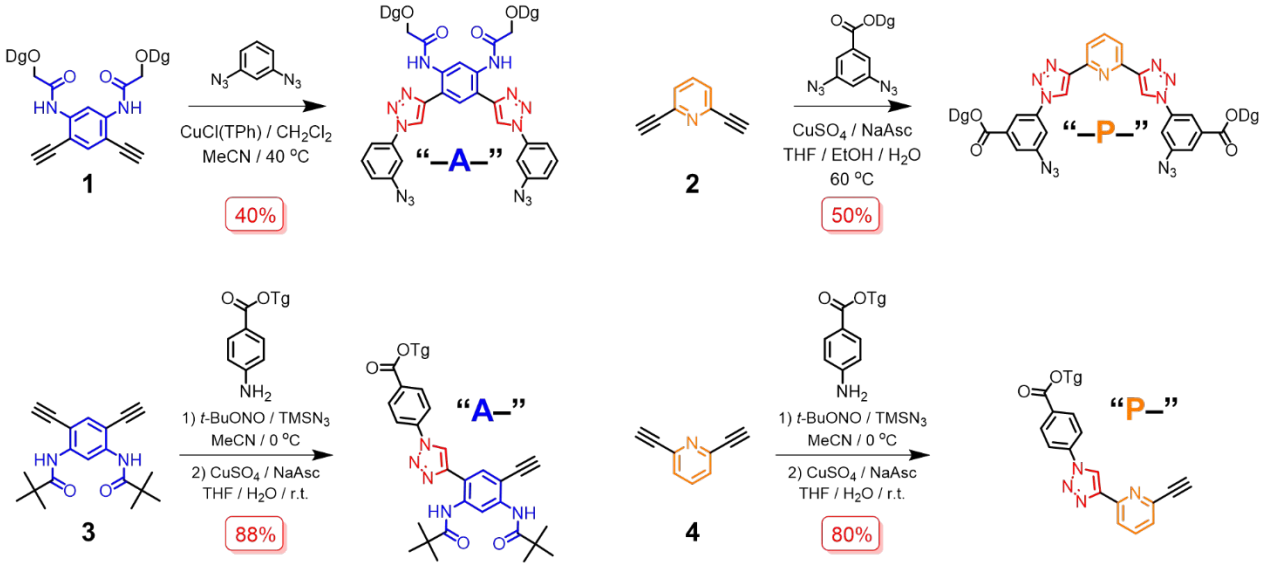

[a]TPh = 1,4-diphenyl-1,2,3-triazol-5-ylidene; TMS = trimethylsilyl.

Stabilization of the double helices is believed to depend on a variety of non-covalent driving forces: the CH•••Cl⁻ hydrogen bonding (Figure 1d–e) and ion-dipole interactions (Figure 1f), just described, as well as π stacking (Figure 1g). Variations in the linear sequence between

the "good" bisamide phenylene and "bad" pyridyl residues can be used to alter the role of these driving forces in controlling the stability of double helices over a pair of single helices.

Scheme 2. Planning Table for the Synthesis of the Sequence-defined Foldamers[a]

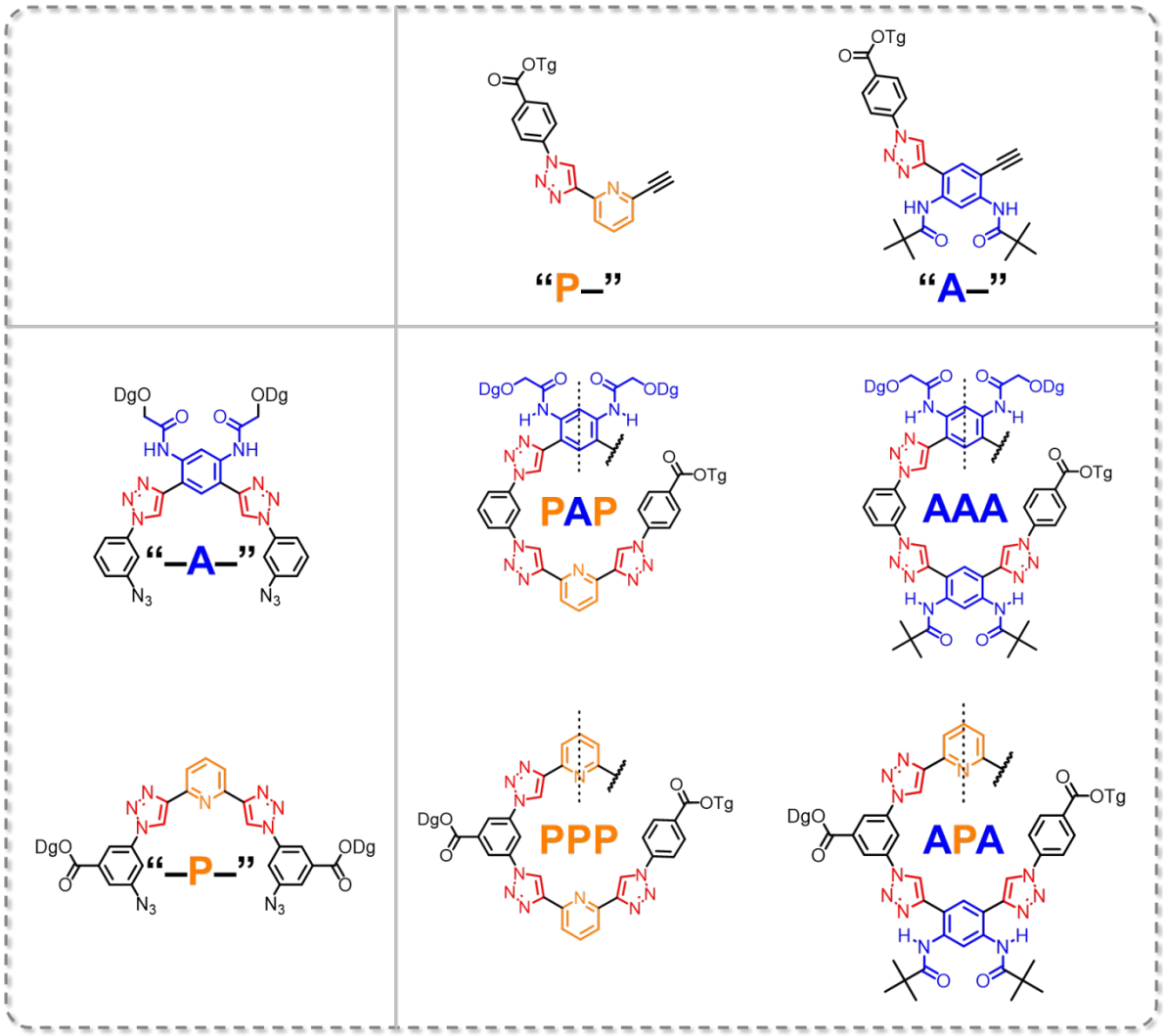

[a]Synthetic conditions: CuI, DBU (1,8-diazabicyclo-(5.4.0)undec-7-ene), PhMe, 60 to 80 °C. Yields: 81% for **PAP**, 75% for **AAA**, 83% for **PPP**, 85% for **APA**.

The foldamers were prepared convergently using Cu(I)-catalyzed azide-alkyne cycloaddition to link building blocks together. The C_2-symmetric sequences were chosen here

for their short synthetic routes, which are easy to modify and their simplified NMR spectra for complete peak assignments. All the bisamides and pyridines incorporated in the synthetic workflow were derived from bis-alkynes (Scheme 1). The foldamers were prepared (Scheme 2) from two equivalents of the appropriate monoalkynyl trimer endgroups with one equivalent of the central bisazido pentamer. The order of introduction of the alkyne-derivitized bisamides and pyridines in the sequences of the foldamers provides access to precise, single-site modifications. Thus, systematic **A↔P** substitutions of the sequence takes advantage of the modular synthesis of the C_2-symmetric aryl-triazole foldamers. The sequence positions subject to substitution (Figure 1d, Schemes S1–S4) are two terminal sites and one central position, generating foldamers with modified sequences designated as follows: **PAP**, **PPP**, **APA**, and **AAA** (Figure 1b).

Characterizations of 1:1 Single and 2:2 Double helix. Initially we saw formation of the single helix with 1:1 stoichiometry, **PAP**•Cl^-, by ^{1}H NMR spectroscopy. Titration of foldamer **PAP** (1 mM, Figure S1) with chloride as the tetraethylammonium salt (TEACl) in dichloromethane shows moderate binding affinity. Consequently, all structural analyses were conducted with excess anion to ensure saturation as the complex. The NMR spectrum (Figure 2a) of the 1:1 complex **PAP**•Cl^- displays an average C_2 symmetry in solution. The downfield shifted positions of the triazole resonances (11.1, 10.2, and 9.6 ppm) confirm hydrogen bonding from all six triazole CH donors to Cl^-. Consistent with other aryl-triazole foldamers,[54-55] sharp proton signals can only be observed after forming the complex. Complete peak assignments were done using 2D ^{1}H-^{1}H ROESY (Figure S6) and DQCOSY (Figure S7). The folded geometry of the 1:1 complex was confirmed by the NOE cross peaks from protons on the terminal phenylenes, H^m, to central triazole CH protons, H^b.

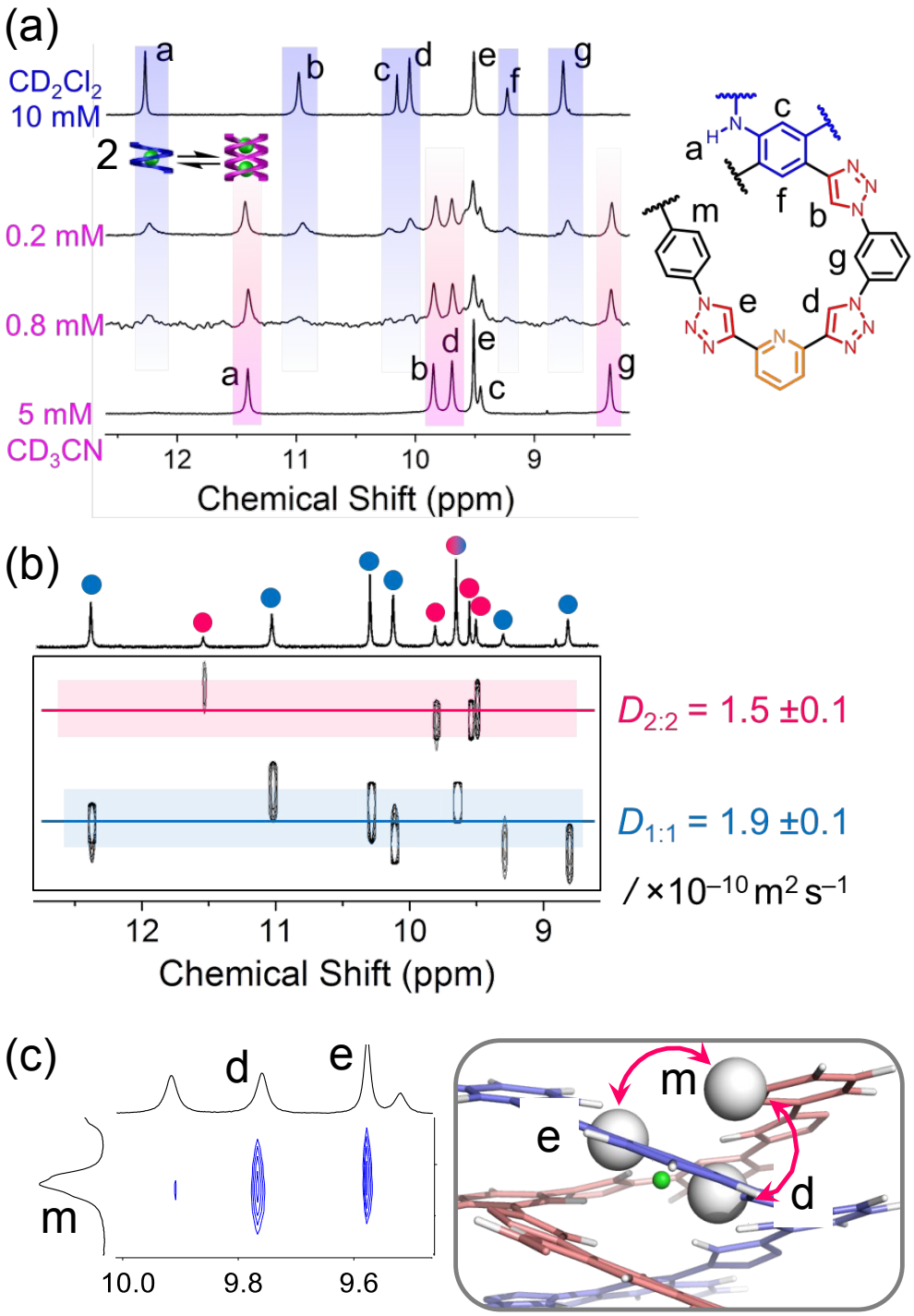

Figure 2. (a) ^{1}H NMR spectra of **PAP** (15 eq. TEACl, 298 K, 500 MHz) in CD_2Cl_2 (5 mM; blue fonts) and CD_3CN (0.2, 0.8, and 5 mM; magenta fonts). Increased number of scans (10,240) was

used to improve the data quality at 0.2 mM. Characterizations of the double helices: (b) DOSY (1,2-$C_2D_4Cl_2$, 5 mM, 15 eq. TEACl, 258 K, 500 MHz, diffusion delay 300 ms, error bars are shown in shades), (c) The inter-strand region in ROESY (CD_3CN, 5 mM, 15 eq. TEACl, 298 K, 500 MHz, mixing time 300 ms) showing spatial proximity unique to double helix based on the DFT-optimized geometry.

Emergence of the double helices was discovered when the foldamer was studied in both polar acetonitrile solvent and in low-temperature nonpolar media. Compared to the room temperature spectrum in dichloromethane (Figure 2a), a new ^{1}H NMR spectrum emerged in acetonitrile with the majority of proton signals shifted upfield. These shifts, together with retention of the overall C_2 symmetry, strongly indicate intertwined helices. The number of intertwining strands was determined to be two as based on diffusion coefficients measured by diffusion-ordered NMR spectroscopy (DOSY; Figure 2b) and using the Stokes-Einstein relationship to calculate the volume ratio (Figure S8). The DOSY measurement was performed in cold 1,2-dichloroethane (DCE) instead of acetonitrile in order to sharpen NMR peaks for more accurate integrals. The involvement of two anions was revealed by high-resolution electrospray ionization, time-of-flight mass spectrometry (ESI-TOF-MS, Figure S26). The ability to include two anions differentiates this newly designed primary sequence from our previous work[29, 54] where only one chloride was hosted by the aryl-triazole double helices. In these previous cases, meta-substituents directed phenyl groups into the top region of the anion-binding cavity to sterically reduce the size of the binding pocket. In the present case, we believe that the para-substituents used with the terminal phenylenes provided sufficient space in the cavity to accommodate two anions.

The 2:2 stoichiometry was supported by a variable-concentration NMR experiment conducted in acetonitrile (Figure 2a). Disassociation of the 2:2 complex into a 1:1 helix upon dilution matches expectation from the associated equilibrium[56] (K_{dim}; Equation 1).

$$(\mathbf{PAP})_2\bullet(Cl^-)_2 \rightleftharpoons 2\ \mathbf{PAP}\bullet Cl^- \qquad K_{dim} \qquad \text{(Eq. 1)}$$

The dimerization constant was determined from the variable-concentration ^{1}H NMR spectra in acetonitrile to be K_{dim} = 13,000 ± 6,000 M^{-1} (log K_{dim} = 4.1 ±0.2).

The water content was found to be relatively constant (0.9 ±0.1% *v*/*v*) for **PAP** in acetonitrile. As a consequence, when we evaluated K_{dim} for **PAP** at two different concentrations, 5 mM and 0.2 mM, the water content increased from being a 20-fold excess relative to the foldamer to 400-fold. Nevertheless, there was no difference in the observed K_{dim}, suggesting water has a negligible role under the condition of our experiments.

The structure of the double helix was further characterized by 2D NMR (Figure 2c) and corroborated with a DFT-optimized geometry of an idealized model (Figure 1g).[57] Spectral features unique to the intertwining geometry of the double helix were identified in the 2D ROESY spectrum. Specifically, we see cross peaks that are possible (HH distances <3.5 Å) in the double helix but are highly unlikely in the single helix (HH distances > 4.6 Å). These all support the DFT structure (Figures 1e and S11–S13).

Stimuli-responsive Interconversion between Single and Double helix. The initial discovery of 2:2 double helices was made by changing solvent or temperature, which also helped identify the external stimuli available for controlling the interconversion between the two

1:1 single helices and the 2:2 double helix. The enhanced stabilization of the 2:2 double helix over the single helix with increasing acetonitrile in chloroform (Figure 3a) suggests that solvophobically-driven π stacking is an essential factor. The population of the double helix increases modestly with polarity until the solvent mixture is dominated by acetonitrile. The enhanced stability of double helices in polar solvents is consistent with burial of a greater number of π surfaces inside the double helix.[29, 42] Deprived of solvent, e.g., during the ESI-TOF-MS experiment, the double helix loses stability even when the sample was injected as concentrated acetonitrile solutions. One difference to prior work with 2:1 double helices of aryl-triazole foldamers around chloride[29] is that the chloride complex of **PAP** allows for double helix formation with solvophobic driving forces in polar aprotic solvents[58] instead of requiring water.

The thermal properties of the 2:2 double helix show the 1:1 helix is favored at elevated temperatures and that the transition temperature (T_c) is solvent-dependent. Upon heating, we see the signature for the double helix gives way to the single helix (Figure 3b). A competing transition could be an unfolding of the helix.[42] On account of the fact that both helices are stabilized by chloride binding, however, the unfolding and loss of the chloride is not observed across the temperatures examined. Consistently, the ^{1}H NMR signature of the 1:1 helix alone is invariant with temperature elevations when examined in DCE (Figures 3b and S14) and in any of the other solvents (Figures S16, S18, and S20). Thus, the transition temperature exclusively corresponds to the thermodynamic signature for exchange between single and double helices.[59]

The 2:2 duplex gained thermal stability in polar solvents (Figure 3c). E.g., the transition temperature increases from –40 ^{o}C in nonpolar DCE to an estimated 100 ^{o}C in acetonitrile; ~20 ^{o}C above the boiling point of the solvent at ambient pressure. Overall, single helices dominate at

room temperature in DCE (log K_{dim} = 1.2 ±0.2) while double helices pervade in polar acetonitrile (log K_{dim} = 4.1 ±1.1).[60]

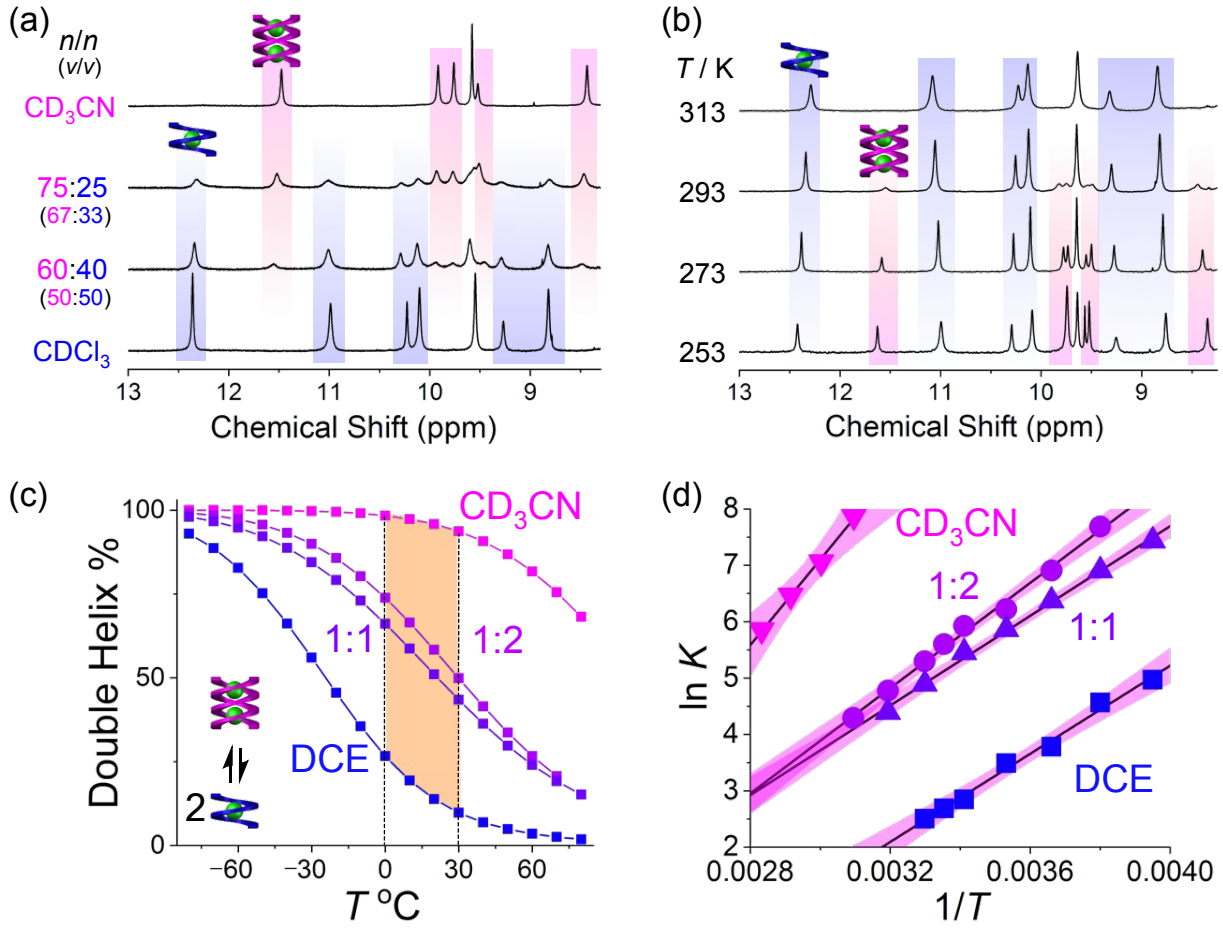

Figure 3. Double helix formation of **PAP** (5 mM, 15 eq. TEACl, 500 MHz) in response to (a) solvent polarity at 298 K, (b) temperature in 1,2-$C_2D_4Cl_2$ (DCE), and (c) two factors combined showing maximal solvent-induced swings in double helix population around ambient temperatures (orange shade). The intermediate solvents are 1:1 DCE:CD_3CN and 1:2 $CDCl_3$:CD_3CN. Curves calculated at 5 mM using corresponding ΔH and $T\,\Delta S$ values (Table 1) from (d) van't Hoff analysis. Shaded areas represent fitting with 99% level of confidence.

The enthalpic and entropic contributions to the dimerization of the single helix into the duplex (Figure 3d; Table 1) were determined by van't Hoff analysis (Section S6).[61] The double helix benefits from enthalpic stabilization and suffers from an entropic penalty. The enthalpic stabilization can be attributed to a greater number of hydrogen bonding interactions and of π-π contacts upon double helix formation while the relatively small entropic penalty is consistent with bringing two helices together into one species. These two factors increase in magnitude with solvent polarity and we see that the growth in the enthalpy contribution dominates. As a consequence, the room temperature data show the single helix dominates in DCE while the duplex dominates in acetonitrile. Therefore, the largest solvent-driven swing in dimerization occurs around room temperature when changing from DCE to acetonitrile.

Table 1. Thermodynamics of single-to-double helix equilibrium in various solvents for **PAP**.[a]

	1,2-$C_2D_4Cl_2$ (DCE)	1:1 DCE:CD_3CN	1:2 $CDCl_3$:CD_3CN	CD_3CN
ΔH^b	–7.8 ±0.6	–7.9 ±0.4	–9.3 ±0.6	–15 ±1
ΔS^c	–21 ±2	–16 ±1	–20 ±2	–31 ±4
ΔG^b	–1.6 ±0.3	–3.0 ±0.4	–3.3 ±0.6	–5.6 ±0.3
log K	1.2 ±0.2	2.2 ±0.3	2.4 ±0.4	4.1 ±0.2
T_c^d	244 ±10	294 ±7	303 ±10	374[e]

[a]Conditions: 5 mM, 15 eq. of TEACl, 298 K. Solvent ratios are indicated in volumes. All errors are presented in 2σ. [b]Unit: kcal mol^{-1}. [c]Unit: cal mol^{-1} K^{-1}. [d]Unit: K. [e]A hypothetical value that exceeds the boiling temperature of acetonitrile at 1 atm.

Single-site Sequence Substitutions (A↔P). Prior anion-bound double helices were found to be either too stable, and therefore largely insensitive to solvent,[22-23, 26] or to be too unstable in solution;[24-25, 27] thus no interconversion was seen. The large solvent response of the 2:2 double helix with foldamer **PAP** is unique. In order to further investigate this behavior, we sought to identify the driving forces governing the stabilization of the double helix using single-site **A↔P** substitutions.

The bisamide phenylene (**A**) and pyridyl (**P**) groups are expected to play complementary roles in stabilizing the helices. These roles can be considered relative to a "blank" sequence consisting of only unsubstituted phenylenes alternating with triazoles.[49] (1) Interactions with anionic guests will be enhanced by **A** residues and impaired with **P** (Figure 1e). (2) The strength of interstrand π stacking, which is only accessible in the double helices, will be tuned by the dipole-dipole interactions between stacked rings. Thus, a π-stacked pair of **AP** residues stabilize the helix with favorable dipole-dipole interactions (Figure 1f), but the double helices will be destabilized when the stacks involve like contacts, e.g., **AA** and **PP**. With the role of these two competing forces in question, we edited the original **PAP** sequence with **A↔P** substitutions as a means to examine which of them dominates stabilization of the double helix and can be used to tune the foldamer's properties.

Systematic **A↔P** substitutions in the original sequence yielded three additional sequences: **PPP**, **APA**, **AAA** (Figure 1a; Scheme 2). The modified sequences were shown to be strong anion receptors in dichloromethane (Figures S3–S5). The apparent binding affinities (Table 2; Figures S37–S40) showed that **PAP** is the weakest and **AAA** is the strongest. The dimerization constant followed a slightly different trend with **APA** being the most stable and

PAP being the least. Interestingly, the high 2:2 stability of foldamers **APA** and **AAA** further allows observation of the 2:1 intermediates (Figures S39 and S40).

Table 2. Apparent stability constants for 1:1 ($K_{1:1}$), 2:1 ($\beta_{2:1}$), and 2:2 ($\beta_{2:2}$) species for all sequences in comparison with the dimerization constant (K_{dim}).[a]

Foldamer	Solvent	**PAP**	**PPP**	**APA**	**AAA**
log $K_{1:1}$	CD_2Cl_2	5.0 ± 0.5	5.5 ± 0.5	6.0 ± 0.5	7.5 ± 0.5
log $\beta_{2:1}$	CD_2Cl_2	-	-	11.0 ± 1.0	11.0 ± 0.5
log $\beta_{2:2}$	CD_2Cl_2	11 ± 1	13 ± 1	17 ± 1	18 ± 1
log K_{dim}	$CDCl_3$	1.2 ±0.2	2.2 ±0.2	4.7 ±0.4	3.2 ±0.3

[a] $K_{1:1}$ represents: $F + Cl^- \rightleftharpoons F{\bullet}Cl^-$; $\beta_{2:1}$ represents: $2\ F + Cl^- \rightleftharpoons F_2{\bullet}Cl^-$; $\beta_{2:2}$ represents: $2\ F + 2\ Cl^- \rightleftharpoons (F{\bullet}Cl^-)_2$; K_{dim} represents: $F{\bullet}Cl^- \rightleftharpoons (F{\bullet}Cl^-)_2$.

The emergence of 2:2 double helices for all new sequences was verified using the chloroform-acetonitrile solvent series (Section S7). The double helix was seen in up-field shifts of proton peaks relative to the single helix (Figures S22–S24), and corroborated by ESI-MS for **PAP** and **AAA**. The stability of the double helix with **PPP** is the lowest and it did not survive in the gas phase (Section S8).

Interrogating Driving Forces based on Sequence Variations. The ^{1}H NMR patterns of 1:1 and 2:2 helical complexes provided well-resolved peak intensities to characterize the impact of sequence variations on solvent-driven stability of the double helices (Figure 4).

We first examined whether solvophobic driving forces are playing a role in stabilizing double helices. Following the methods developed by others[58, 62-70] to diagnose the solvophobic effect we changed the solvent quality from good (chloroform) to bad (acetonitrile). We saw that all the foldamer sequences have their equilibrium shifted from single to double helices in acetonitrile. Similar approaches have been used before for other aryl-triazole foldamers: in one case the amount of water was increased in acetonitrile to favor a chloride-stabilized 2:1 double helix over a single helix,[29] and in another the amount of acetonitrile was increased in THF to drive folding.[55] These aryl-triazole foldamers all showed the classic signature for the solvophobic effect despite differences in the sequence and aromatic compositions. That is, poor solvents help promote burial of π surfaces and consequently the folding of aryl-triazole foldamers and the formation of double helices.

While it may seem unusual for the solvophobic driving forces to apply to π surfaces as polar as triazoles and pyridines (5 and 2 Debye dipoles, respectively), similar findings have been reported by Diederich,[62-63] Cram,[64] Moore,[58, 66] Hunter,[65, 68] Huc,[67] and Cockroft.[69-70] The aromatic rings examined in those reports, e.g., methoxylbenzene,[63] nitrodiazines,[64] and benzoate esters,[58] also carry dipole moments ranging from 2 to 5 Debye.

Finally, the total π surface areas remain the same between sequences we examined herein. Thus, the solvophobic effect must be considered as a background factor for all the foldamers on top of which we see a sequence dependence (Figure 4), which must also be evaluated.

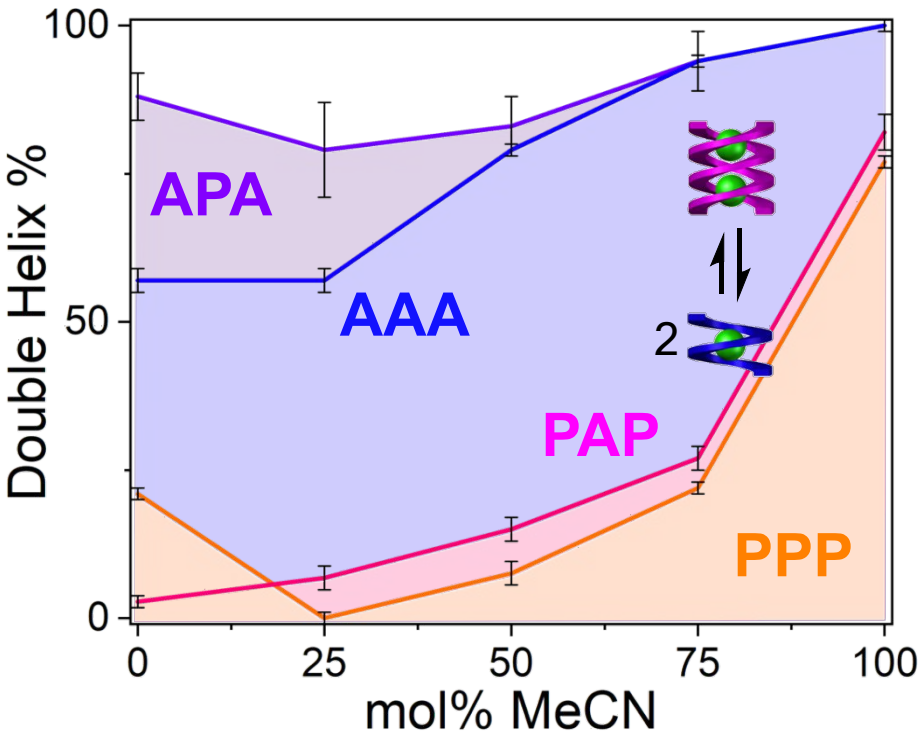

Figure 4. ^{1}H The phase diagram of double helix population *vs*. solvent polarity for **PPP**, **PAP**, **APA**, and **AAA** (1 mM, 298 K).

To our surprise, we find that the significant differences in the dimerization stability of double helix between sequences are dictated by anion binding, not dipolar stacking.[71] The phase diagram shows big differences between two pairs of sequences separated by the large blue gap in Figure 4. First consider the expectation that increasingly polar solvent mixtures will enhance π-stacking. We would thus expect for a mixture of **P** and **A** residues in the sequence to produce the **PA** stacks and contribute greater stability than **PP** or **AA** stacks. If dipolar stacking dominated, the **APA** and **PAP** sequences should have a stability gap relative to **AAA** and **PPP**. This is not what we see. Instead, the stability difference is determined by the identity of the terminal residues; the large blue gap in the phase diagram separates the **A**X**A** from **P**X**P** sequences. Despite these differences, double helix stability was also found to be enhanced with

solvophobically-driven π stacking as the solvent mixture was made more polar; nevertheless, anion-stabilization still dominated at the end with the 20% difference between **A**X**A** and **P**X**P**.

We also considered the role of anion-anion repulsions on the stability of the double helix. We expected that the double helix would be more stable when the anions were further apart, as measured from the DFT-optimized structures. We see sequence variations in the Cl^{-}•••Cl^{-} distances, with the shortest corresponding to the weakest double helix, **PAP** at 4.7 Å; a distance that is longer than the sum of the vdW radii of 3.5 Å, but similar to Maeda's 2:2 Cl^{-} complex in the solid state (4.6 Å).[27] Nevertheless, there is no clear correlation between the inter-anion distances and log K_{dim}. Instead, a more complex relationship emerges in which we find that duplex stability depends on sequence.

The location of the stabilizing residues within the sequence also matters. Double helices can be biased over singles by strategically placing favorable CH•••Cl^{-} contacts near the end of the sequence, i.e., substituting **P** residues with **A** residues at the terminal sites. For example, we observed a dramatic enhancement in stability on going from **P**X**P** to **A**X**A**, (X = **P** or **A**); whereas substitutions in the central residues failed to provide significant improvements from **P<u>P</u>P** to **P<u>A</u>P** and even lowered the stability from **A<u>P</u>A** to **A<u>A</u>A** in nonpolar solvents (Figure 4).

Instead of being dominated by anion-anion repulsions, we found a strong correlation between the stability of double helices and the electrostatic stabilization of anions inside the helices. DFT calculation shows that formation of every double helix enhances the electrostatic potentials (ESP; Figures S29–S36) at the Cl^{-} binding sites relative to their respective single helix (ΔESP = 18 – 60 kJ mol^{-1}; Table S2). This enhancement is more significant (Figure 5a) when the terminal residue is **A** rather than **P** and attributed to favorable and unfavorable anion stabilization, respectively. We see that a larger increase in ESP (ΔESP) upon dimerization enhances the

stability of the double helix (log K_{dim}) in a low dielectric solvent, chloroform, where electrostatics dominates.[53,72,73]

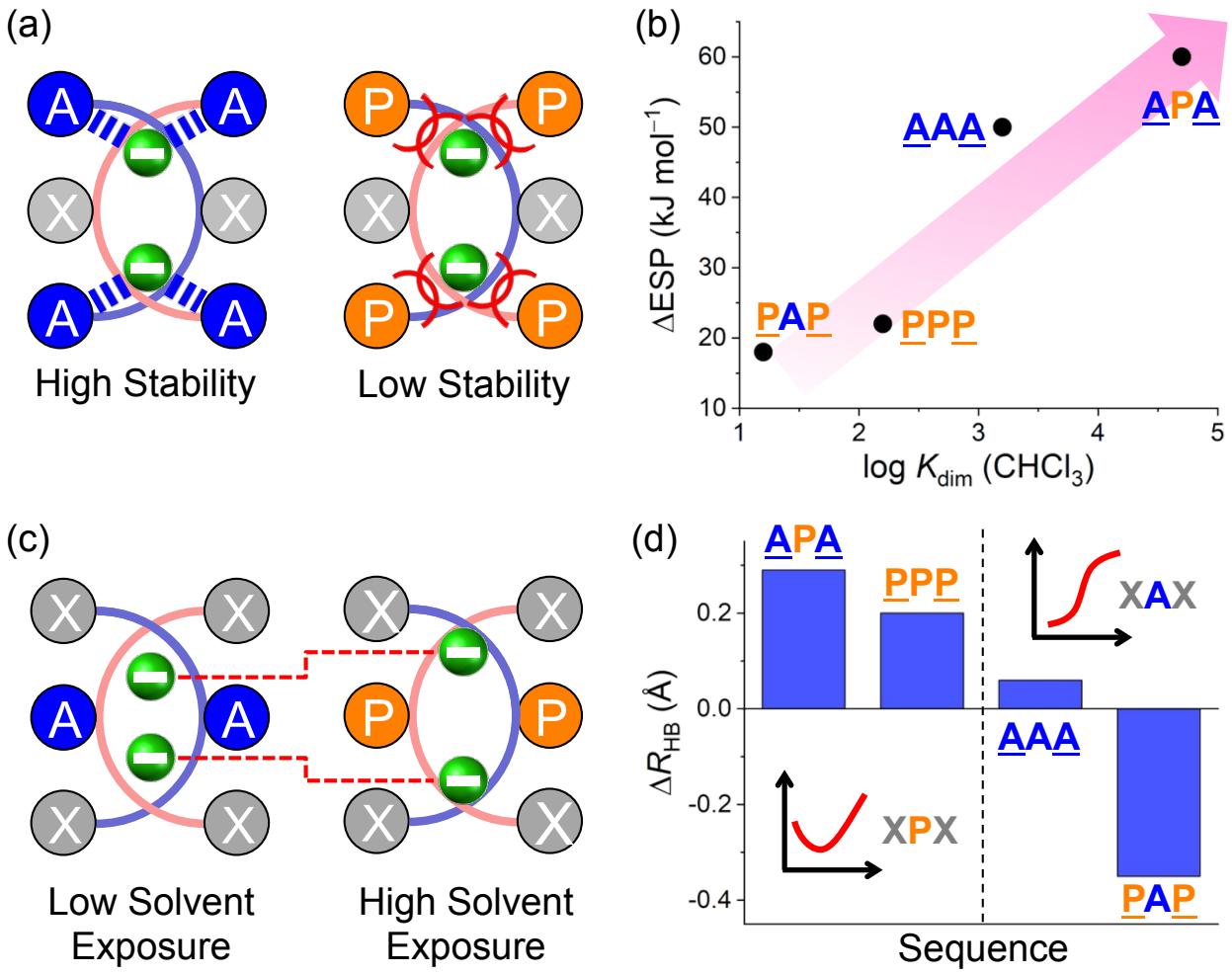

Figure 5. (a) The stabilization (log K_{dim}) is greater for A-terminated sequences, correlating with (b) the enhancement in electrostatic potential ($\Delta ESP = ESP_{2:2} - ESP_{1:1}$) upon dimerization. (c) The solvent exposure is higher for P-centered sequences, correlating with (d) longer HB distances to the central donors, $\Delta R_{HB} = \Delta R_{HB}$ (central site: CH•••Cl⁻) – ΔR_{HB} (terminal site: CH•••Cl⁻).

We also evaluated the impact of the deformation energy penalty that is incurred during the formation of double helices from single helices by using the calculated geometries. Among the various deformations is the expansion of torsion angles[43] known to be a considerable enthalpic cost to double helix formation. While we might expect higher deformation penalty to result in lower stability of the double helix, we found no linear correlation between deformation energy and the relative stability of the double and single helices (see Table S3).

Interestingly, the stability of P-centered sequences (**A<u>P</u>A** and **P<u>P</u>P**) displayed a U-shaped solvent dependence (Figure 4); in contrast, the stability of **A<u>A</u>A** and **P<u>A</u>P** show a simple correlation with stability following solvent polarity. A similar U-shape in solvent dependence was seen by Hamilton when folding a 17-residue peptide[74] by increasing water in trifluoroethanol. Hamilton reasoned that this U-shaped dependence emerged from the competing roles that the two solvents have on the driving forces: the loss of hydrogen bonds upon partial hydration is compensated for by the hydrophobic effect upon further addition of water. Huc also observed the weakening of double helices that are preorganized by intramolecular hydrogen bonding when the polarity of the solvent is increased,[43] and that the weakening occurs despite the underlying importance of intramolecular π-π stacking. Presumably, the same applies for **A<u>P</u>A** and **P<u>P</u>P**. The initial loss in stability with addition of 25% acetonitrile may arise from the increasing dielectric constant that impairs the CH•••Cl^- hydrogen bonds.[53] One might also expect the Cl^-•••Cl^- and pyridine•••Cl^- repulsions to be weakened; but these interactions are buried deeper inside the cylindrical cavity of the double helices and are less exposed to solvent than the CH•••Cl^- interactions (Figures 5a and 5c). As a result, the loss in hydrogen bonding strength is still expected to dominate the solvent dependence of **APA** and **PPP**. As the acetonitrile content is

increased further and surpasses 50%, however, solvophobic driving forces increase to help stabilize the double helix and are then able to compensate for the weaker hydrogen bonding.

We only see this behavior with **P**-centered sequences suggesting they are more susceptible to dielectric screening by the solvent than **A**-centered ones. DFT calculation shows that when a **P** residue is present in the central residue, Cl^- anions are more exposed to the solvent environment (Figure 5c). This higher exposure is reflected in the longer CH•••Cl^- hydrogen bonds seen with the central residues than with those involving terminal residues (Figure 5d; a positive ΔR_{HB}). The fact that the important terminal donors (Figure 5a) are more exposed to the solvent agrees with the higher dielectric susceptibility seen in the **P**-centered sequences.

CONCLUSIONS

We demonstrated that interconversion between chloride-stabilized double and single helices can be both understood and controlled by sequence modification strategies. Switching from the 1:1 single helix to the 2:2 duplex at room temperature could be promoted with solvents of greater polarity. Single-site **A**↔**P** substitutions on three synthetically accessible positions were applied in the sequence to understand these trends. We found that while solvophobically-driven π stacking is essential, the inclusion and location of anion-stabilizing (**A**) and anion-destabilizing (**P**) residues dictate the stability differences between sequences and their different solvent-dependences. We found that the double helices dominate over single helices when the stabilizing **A** residue is present at the ends. The stability profile of **P**-centered sequences has a U-shape dependence on solvent polarity that likely reflects the details of the anionic guest‘s location relative to the solvent environment. Overall, we

anticipate that the 2:2 anion-templated double helices will provide a useful platform to understand how abiological sequence controls the emergence of complex structures and functions.[75] Being able to encode information by placing residues at different locations of the sequence provides a powerful tool for controlling strutcure and properties of abiological foldamers.

ASSOCIATED CONTENT

Supporting Information

Supporting Information is available free of charge on the ACS Publications website at DOI: 10.1021/jacs.XXXXXXX.

Coordinates for the 4 single helices and the 4 double helices (**MOL**)

Compound synthesis and characterization, titration, variable-temperature NMR, variable-solvent analysis, and NMR spectra (**PDF**)

AUTHOR INFORMATION

Corresponding Authors

*yl41@indiana.edu

*aflood@indiana.edu

Present Address

‡Beckman Institute for Advanced Science and Technology, University of Illinois at Urbana-Champaign, 405 North Mathews Avenue, Urbana, IL 61801, USA.

Notes

The authors declare no competing financial interest.

ACKNOWLEDGMENTS

This work was supported by the Chemical Sciences, Geosciences and Biosciences Division, Office of Basic Energy Sciences, Office of Science, U.S. Department of Energy (DE-FG02-09ER16068).

REFERENCES

1. Modi, S.; Nizak, C.; Surana, S.; Halder, S.; Krishnan, Y. Two DNA nanomachines map pH changes along intersecting endocytic pathways inside the same cell. *Nat. Nanotechnol.* **2013,** *8*, 459–467.
2. Edwardson, T. G.; Lau, K. L.; Bousmail, D.; Serpell, C. J.; Sleiman, H. F. Transfer of molecular recognition information from DNA nanostructures to gold nanoparticles. *Nat. Chem.* **2016,** *8*, 162–170.
3. Ong, L. L.; Hanikel, N.; Yaghi, O. K.; Grun, C.; Strauss, M. T.; Bron, P.; Lai-Kee-Him, J.; Schueder, F.; Wang, B.; Wang, P.; Kishi, J. Y.; Myhrvold, C.; Zhu, A.; Jungmann, R.; Bellot, G.; Ke, Y.; Yin, P. Programmable self-assembly of three-dimensional nanostructures from 10,000 unique components. *Nature* **2017,** *552*, 72–77.
4. Tikhomirov, G.; Petersen, P.; Qian, L. Fractal assembly of micrometre-scale DNA origami arrays with arbitrary patterns. *Nature* **2017,** *552*, 67–71.
5. Wagenbauer, K. F.; Sigl, C.; Dietz, H. Gigadalton-scale shape-programmable DNA assemblies. *Nature* **2017,** *552*, 78–83.
6. Goto, H.; Furusho, Y.; Yashima, E. Double helical oligoresorcinols specifically recognize oligosaccharides via heteroduplex formation through noncovalent interactions in water. *J. Am. Chem. Soc.* **2007,** *129*, 9168–9174.
7. Gan, Q.; Wang, X.; Kauffmann, B.; Rosu, F.; Ferrand, Y.; Huc, I. Translation of rod-like template sequences into homochiral assemblies of stacked helical oligomers. *Nat. Nanotechnol.* **2017,** *12*, 447–452.
8. Jia, C.; Zuo, W.; Yang, D.; Chen, Y.; Cao, L.; Custelcean, R.; Hostas, J.; Hobza, P.; Glaser, R.; Wang, Y. Y.; Yang, X. J.; Wu, B. Selective binding of choline by a phosphate-coordination-based triple helicate featuring an aromatic box. *Nat. Commun.* **2017,** *8*, 938.
9. Miwa, K.; Furusho, Y.; Yashima, E. Ion-triggered spring-like motion of a double helicate accompanied by anisotropic twisting. *Nat. Chem.* **2010,** *2*, 444–449.
10. Ferrand, Y.; Gan, Q.; Kauffmann, B.; Jiang, H.; Huc, I. Template-induced screw motions within an aromatic amide foldamer double helix. *Angew. Chem. Int. Ed.* **2011,** *50*, 7572–7575.
11. Gan, Q.; Ferrand, Y.; Bao, C.; Kauffmann, B.; Grelard, A.; Jiang, H.; Huc, I. Helix-rod host-guest complexes with shuttling rates much faster than disassembly. *Science* **2011,** *331*, 1172–1175.
12. Shigeno, M.; Kushida, Y.; Yamaguchi, M. Heating/cooling stimulus induces three-state molecular switching of pseudoenantiomeric aminomethylenehelicene oligomers: reversible nonequilibrium thermodynamic processes. *J. Am. Chem. Soc.* **2014,** *136*, 7972–7980.
13. Suzuki, Y.; Nakamura, T.; Iida, H.; Ousaka, N.; Yashima, E. Allosteric regulation of unidirectional spring-like motion of double-stranded helicates. *J. Am. Chem. Soc.* **2016,** *138*, 4852–4859.
14. Zhao, D.; van Leeuwen, T.; Cheng, J.; Feringa, B. L. Dynamic control of chirality and self-assembly of double-stranded helicates with light. *Nat. Chem.* **2017,** *9*, 250–256.
15. Wang, X.; Wicher, B.; Ferrand, Y.; Huc, I. Orchestrating directional molecular motions: kinetically controlled supramolecular pathways of a helical host on rodlike guests. *J. Am. Chem. Soc.* **2017,** *139*, 9350–9358.

16. Yamada, H.; Furusho, Y.; Yashima, E. Diastereoselective imine-bond formation through complementary double-helix formation. *J. Am. Chem. Soc.* **2012,** *134*, 7250–7253.
17. Y. Liu; Flood, A. H., Synergistic effects in double helical foldamers. In *Synergy in Supramolecular Chemistry*; Nabeshima, T., Ed.; CRC Press: Boca Raton, 2014; 149–172.
18. Albrecht, M. "Let's twist again" – double-stranded, triple-stranded, and circular helicates. *Chem. Rev.* **2001,** *101*, 3457–3498.
19. Piguet, C.; Borkovec, M.; Hamacek, J.; Zeckert, K. Strict self-assembly of polymetallic helicates: the concepts behind the semantics. *Coord. Chem. Rev.* **2005,** *249*, 705–726.
20. Yashima, E.; Ousaka, N.; Taura, D.; Shimomura, K.; Ikai, T.; Maeda, K. Supramolecular helical systems: Helical assemblies of small molecules, foldamers, and polymers with chiral amplification and their functions. *Chem. Rev.* **2016,** *116*, 13752–13990.
21. He, Q.; Tu, P.; Sessler, J. L. Supramolecular chemistry of anionic dimers, trimers, tetramers and clusters. *Chem* **2018,** *4*, 46–93.
22. Sánchez-Quesada, J.; Seel, C.; Prados, P.; de Mendoza, J.; Dalcol, I.; Giralt, E. Anion helicates: Double strand helical self-assembly of chiral bicyclic guanidinium dimers and tetramers around sulfate templates. *J. Am. Chem. Soc.* **1996,** *118*, 277–278.
23. Massena, C. J.; Wageling, N. B.; Decato, D. A.; Martin Rodriguez, E.; Rose, A. M.; Berryman, O. B. A halogen-bond-induced triple helicate encapsulates iodide. *Angew. Chem. Int. Ed.* **2016,** *55*, 12398–12402.
24. Keegan, J.; Kruger, P. E.; Nieuwenhuyzen, M.; O'Brien, J.; Martin, N. Anion directed assembly of a dinuclear double helicate. *Chem. Commun.* **2001**, 2192–2193.
25. Coles, S. J.; Frey, J. G.; Gale, P. A.; Hursthouse, M. B.; Light, M. E.; Navakhun, K.; Thomas, G. L. Anion-directed assembly: the first fluoride-directed double helix. *Chem. Commun.* **2003**, 568–569.
26. Li, S.; Jia, C.; Wu, B.; Luo, Q.; Huang, X.; Yang, Z.; Li, Q. S.; Yang, X. J. A triple anion helicate assembled from a bis(biurea) ligand and phosphate ions. *Angew. Chem. Int. Ed.* **2011,** *50*, 5721–5724.
27. Haketa, Y.; Maeda, H. From helix to macrocycle: Anion-driven conformation control of π-conjugated acyclic oligopyrroles. *Chem. Eur. J.* **2011,** *17*, 1485–1492.
28. Maeda, H.; Kitaguchi, K.; Haketa, Y. Anion-responsive covalently linked and metal-bridged oligomers. *Chem. Commun.* **2011,** *47*, 9342–9344.
29. Hua, Y.; Liu, Y.; Chen, C. H.; Flood, A. H. Hydrophobic collapse of foldamer capsules drives picomolar-level chloride binding in aqueous acetonitrile solutions. *J. Am. Chem. Soc.* **2013,** *135*, 14401–14412.
30. Prince, R. B.; Barnes, S. A.; Moore, J. S. Foldamer-based molecular recognition. *J. Am. Chem. Soc.* **2000,** *122*, 2758–2762.
31. Suk, J. M.; Naidu, V. R.; Liu, X.; Lah, M. S.; Jeong, K. S. A foldamer-based chiroptical molecular switch that displays complete inversion of the helical sense upon anion binding. *J. Am. Chem. Soc.* **2011,** *133*, 13938–13941.
32. Sanford, A.; Gong, B. Evolution of helical foldamers. *Curr. Org. Chem.* **2003,** *7*, 1649–1659.
33. Steinwand, S.; Yu, Z.; Hecht, S.; Wachtveitl, J. Ultrafast dynamics of photoisomerization and subsequent unfolding of an oligoazobenzene foldamer. *J. Am. Chem. Soc.* **2016,** *138*, 12997–13005.

34. De Poli, M.; Zawodny, W.; Quinonero, O.; Lorch, M.; Webb, S. J.; Clayden, J. Conformational photoswitching of a synthetic peptide foldamer bound within a phospholipid bilayer. *Science* **2016,** *352*, 575–580.
35. Jeon, H. G.; Lee, H. K.; Lee, S.; Jeong, K. S. Foldamer-based helicate displaying reversible switching between two distinct conformers. *Chem. Commun.* **2018,** *54*, 5740–5743.
36. Valderrey, V.; Escudero-Adan, E. C.; Ballester, P. Polyatomic anion assistance in the assembly of [2]pseudorotaxanes. *J. Am. Chem. Soc.* **2012,** *134*, 10733–10736.
37. Howe, E. N.; Bhadbhade, M.; Thordarson, P. Cooperativity and complexity in the binding of anions and cations to a tetratopic ion-pair host. *J. Am. Chem. Soc.* **2014,** *136*, 7505–7516.
38. Fatila, E. M.; Twum, E. B.; Sengupta, A.; Pink, M.; Karty, J. A.; Raghavachari, K.; Flood, A. H. Anions stabilize each other inside macrocyclic hosts. *Angew. Chem. Int. Ed.* **2016,** *55*, 14057–14062.
39. Bilbeisi, R. A.; Prakasam, T.; Lusi, M.; El Khoury, R.; Platas-Iglesias, C.; Charbonniere, L. J.; Olsen, J. C.; Elhabiri, M.; Trabolsi, A C–H•••anion interactions mediate the templation and anion binding properties of topologically non-trivial metal-organic structures in aqueous solutions. *Chem. Sci.* **2016,** *7*, 2524–2531.
40. Mungalpara, D.; Valkonen, A.; Rissanen, K.; Kubik, S. Efficient stabilisation of a dihydrogenphosphate tetramer and a dihydrogenpyrophosphate dimer by a cyclic pseudopeptide containing 1,4-disubstituted 1,2,3-triazole moieties. *Chem. Sci.* **2017,** *8*, 6005–6013.
41. He, Q.; Kelliher, M.; Bahring, S.; Lynch, V. M.; Sessler, J. L. A Bis-calix[4]pyrrole enzyme mimic that constrains two oxoanions in close proximity. *J. Am. Chem. Soc.* **2017,** *139*, 7140–7143.
42. Goto, H.; Furusho, Y.; Miwa, K.; Yashima, E. Double helix formation of oligoresorcinols in water: thermodynamic and kinetic aspects. *J. Am. Chem. Soc.* **2009,** *131*, 4710–4719.
43. Berni, E.; Kauffmann, B.; Bao, C.; Lefeuvre, J.; Bassani, D. M.; Huc, I. Assessing the mechanical properties of a molecular spring. *Chem. Eur. J.* **2007,** *13*, 8463–8469.
44. Haldar, D.; Jiang, H.; Leger, J. M.; Huc, I. Interstrand interactions between side chains in a double-helical foldamer. *Angew. Chem. Int. Ed.* **2006,** *45*, 5483–5486.
45. De, S.; Chi, B.; Granier, T.; Qi, T.; Maurizot, V.; Huc, I. Designing cooperatively folded abiotic uni- and multimolecular helix bundles. *Nat. Chem.* **2018,** *10*, 51–57.
46. Garric, J.; Leger, J. M.; Huc, I. Molecular apple peels. *Angew. Chem. Int. Ed.* **2005,** *44*, 1954–1958.
47. Chandramouli, N.; Ferrand, Y.; Lautrette, G.; Kauffmann, B.; Mackereth, C. D.; Laguerre, M.; Dubreuil, D.; Huc, I. Iterative design of a helically folded aromatic oligoamide sequence for the selective encapsulation of fructose. *Nat. Chem.* **2015,** *7*, 334–341.
48. Li, Y.; Flood, A. H. Pure C-H hydrogen bonding to chloride ions: a preorganized and rigid macrocyclic receptor. *Angew. Chem. Int. Ed.* **2008,** *47*, 2649–2652.
49. Li, Y.; Flood, A. H. Strong, size-selective, and electronically tunable C–H•••halide binding with steric control over aggregation from synthetically modular, shape-persistent [3_4]triazolophanes. *J. Am. Chem. Soc.* **2008,** *130*, 12111–12122.
50. Hua, Y.; Ramabhadran, R. O.; Uduehi, E. O.; Karty, J. A.; Raghavachari, K.; Flood, A. H. Aromatic and aliphatic CH hydrogen bonds fight for chloride while competing alongside ion pairing within triazolophanes. *Chem. Eur. J.* **2011,** *17*, 312–321.

51. Ramabhadran, R. O.; Liu, Y.; Hua, Y.; Ciardi, M.; Flood, A. H.; Raghavachari, K. An overlooked yet ubiquitous fluoride congenitor: binding bifluoride in triazolophanes using computer-aided design. *J. Am. Chem. Soc.* **2014,** *136*, 5078–5089.
52. Lee, S.; Hirsch, B. E.; Liu, Y.; Dobscha, J. R.; Burke, D. W.; Tait, S. L.; Flood, A. H. Multifunctional tricarbazolo triazolophane macrocycles: One-pot preparation, anion binding, and hierarchical self-organization of multilayers. *Chem. Eur. J.* **2016,** *22*, 560–569.
53. Liu, Y.; Sengupta, A.; Raghavachari, K.; Flood, A. H. Anion binding in solution: Beyond the electrostatic regime. *Chem* **2017,** *3*, 411–427.
54. Hua, Y.; Flood, A. H. Flipping the switch on chloride concentrations with a light-active foldamer. *J. Am. Chem. Soc.* **2010,** *132*, 12838-12840.
55. Lee, S.; Hua, Y.; Flood, A. H. beta-sheet-like hydrogen bonds interlock the helical turns of a photoswitchable foldamer to enhance the binding and release of chloride. *J. Org. Chem.* **2014,** *79*, 8383–8396.
56. The conversion of a 2:1 complex into two equivalents of the 1:1 complex in the presence of excess chloride is concentration independent, which is not what we observe.
57. Attempts to grow crystals have not yielded a diffraction-quality sample suitable for X-ray structural analysis.
58. Nelson, J. C.; Saven, J. G.; Moore, J. S.; Wolynes, P. G. Solvophobically driven folding of nonbiological oligomers. *Science* **1997,** *277*, 1793–1796.
59. The transition temperature, T_c, is defined as the temperature under which half population of foldamer is present as the 1:1 single helix.
60. For reference, a 50:50 single:double helix equilibrium position at 5 mM total foldamer concentration corresonds to a log $K_{dim} = 2.3$.
61. Chloroform was replaced by 1,2-dichloroethane in order to access a wider temperature range; the replacement is expected to have minimal impact as both solvents have similar polarity on the normalized $E_T(30)$ scale: 0.26 vs 027.
62. Smithrud, D. B.; Diederich, F. Strength of molecular complexation of apolar solutes in water and in organic solvents is predictable by linear free energy relationships: A general model for solvation effects on apolar binding. *J. Am. Chem. Soc.* **1990,** *112*, 339–343.
63. Smithrud, D. B.; Sanford, E. M.; Chao, I.; Ferguson, S. B.; Carcanague, D. R.; Evanseck, J. D.; Houk, K. N.; Diederich, F. Solvent effects in molecular recognition. *Pure Appl. Chem.* **1990,** *62*, 2227–2236.
64. Cram, D. J.; Choi, H. J.; Bryant, J. A.; Knobler, C. B. Host-guest complexation. 62. Solvophobic and entropic driving forces for forming velcraplexes, which are 4-fold, lock-key dimers in organic media. *J. Am. Chem. Soc.* **1992,** *114*, 7748–7765.
65. Breault, G. A.; Hunter, C. A.; Mayers, P. C. Influence of solvent on aromatic interactions in metal tris-bipyridine complexes. *J. Am. Chem. Soc.* **1998,** *120*, 3402–3410.
66. Prince, R. B.; Okada, T.; Moore, J. S. Controlling the secondary structure of nonbiological oligomers with solvophobic and coordination interactions. *Angew. Chem. Int. Ed.* **1999,** *38*, 233–236.
67. Berl, V. V.; Krische, M. J.; Huc, I. I.; Lehn, J. M.; Schmutz, M. Template-induced and molecular recognition directed hierarchical generation of supramolecular assemblies from molecular strands. *Chem. Eur. J.* **2000,** *6*, 1938–1946.
68. Hunter, C. A. Quantifying intermolecular interactions: guidelines for the molecular recognition toolbox. *Angew. Chem. Int. Ed.* **2004,** *43*, 5310–5324.

69. Adam, C.; Yang, L.; Cockroft, S. L. Partitioning solvophobic and dispersion forces in alkyl and perfluoroalkyl cohesion. *Angew. Chem. Int. Ed.* **2015,** *127*, 1180–1183.
70. Yang, L.; Adam, C.; Cockroft, S. L. Quantifying solvophobic effects in nonpolar cohesive interactions. *J. Am. Chem. Soc.* **2015,** *137*, 10084–10087.
71. Li, Y.; Pink, M.; Karty, J. A.; Flood, A. H. Dipole-promoted and size-dependent cooperativity between pyridyl-containing triazolophanes and halides leads to persistent sandwich complexes with iodide. *J. Am. Chem. Soc.* **2008,** *130*, 17293–17295.
72. The correlation between electrostatics and binding differentials are seen here for two highly related states of the same receptor. In general, electrostatics is not the ideal predictor of absolute anion binding stability. See reference 73.
73. Sengupta, A.; Liu, Y.; Flood, A. H.; Raghavachari, K. Anion-binding macrocycles operate beyond the electrostatic regime: Interaction distances matter. *Chem. Eur. J.* **2018,** *24*, 14409–14417.
74. Albert, J. S.; Hamilton, A. D. Stabilization of helical domains in short peptides using hydrophobic interactions. *Biochemistry* **2002,** *34*, 984–990.
75. Lutz, J. F.; Ouchi, M.; Liu, D. R.; Sawamoto, M. Sequence-controlled polymers. *Science* **2013,** *341*, 1238149.

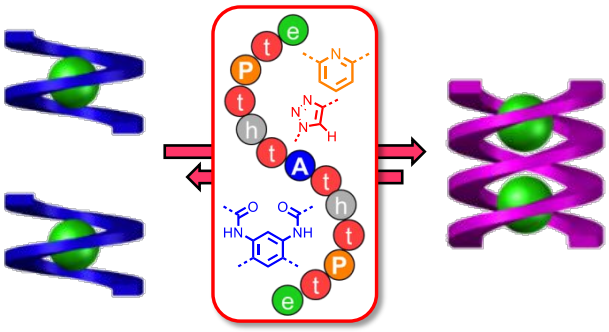

TOC Graphic